Published in final edited form as:

Clin Cancer Res. 2016 July 15; 22(14): 3683–3694. doi:10.1158/1078-0432.CCR-15-2323.

Pharmacodynamic Response of the MET/HGF-Receptor to Small Molecule Tyrosine Kinase Inhibitors Examined with Validated, Fit-for-Clinic Immunoassays

Apurva K Srivastava[1], **Melinda G. Hollingshead**[2], **Jennifer Weiner**[1], **Tony Navas**[1], **Yvonne A. Evrard**[1], **Sonny Khin**[1], **Jiuping Ji**[3], **Yiping Zhang**[3], **Suzanne Borgel**[4], **Thomas D Pfister**[1], **Robert J. Kinders**[1], **Donald P Bottaro**[5], **W Marston Linehan**[5], **Joseph E Tomaszewski**[6], **James H Doroshow**[6], **Ralph E Parchment**[1,*]

[1]Laboratory of Human Toxicology and Pharmacology, Applied/Developmental Research Directorate, Leidos Biomedical Research, Inc., Frederick National Laboratory for Cancer Research, Frederick, Maryland, 21702

[2]Biological Testing Branch, Developmental Therapeutics Program, Frederick National Laboratory for Cancer Research, Frederick, Maryland, 21702

[3]National Clinical Target Validation Laboratory, Applied/Developmental Research Directorate, Leidos Biomedical Research, Inc., Frederick National Laboratory for Cancer Research, Frederick, Maryland, 21702

[4]In Vivo Evaluation Group, Applied/Developmental Research Directorate, Leidos Biomedical Research, Inc., Frederick National Laboratory for Cancer Research, Frederick, Maryland, 21702

[5]Urologic Oncology Branch, National Cancer Institute, Bethesda, Maryland, 20892

[6]Division of Cancer Treatment and Diagnosis, National Cancer Institute, Bethesda, MD 20892

Abstract

Purpose: Rational development of targeted MET inhibitors for cancer treatment requires a quantitative understanding of target pharmacodynamics, including molecular target engagement, mechanism of action, and duration of effect.

Methods: Sandwich immunoassays and specimen-handling procedures were developed and validated for quantifying full-length MET and its key phosphospecies (pMET) in core tumor biopsies. MET was captured using an antibody to the extracellular domain and then probed using antibodies to its C-terminus (full-length) and epitopes containing pY1234/1235, pY1235, and pY1356. Using pMET:MET ratios as assay endpoints, MET inhibitor pharmacodynamics were characterized in MET-amplified and -compensated (VEGFR blockade) models.

Results: By limiting cold ischemia time to less than two min, the pharmacodynamic effects of the MET inhibitors PHA665752 and PF02341066 (crizotinib) were quantifiable using core needle

[*]**Corresponding Author**: Ralph E. Parchment, Laboratory of Human Toxicology and Pharmacology, Leidos Biomedical Research, Inc., Frederick National Laboratory of Cancer Research, PO Box B, Frederick, MD 21702. Phone: (301) 846-5427; parchmentr@mail.nih.gov.

Disclosure of Potential Conflicts of Interest: None.

biopsies of human gastric carcinoma xenografts (GTL-16 and SNU5). One dose decreased pY1234/1235 MET:MET, pY1235-MET:MET, and pY1356-MET:MET ratios by 60%-80% within 4 h, but this effect was not fully sustained despite continued daily dosing. VEGFR blockade by pazopanib increased pY1235-MET:MET and pY1356-MET:MET ratios, which was reversed by tivantinib. Full-length MET was quantifiable in 5 of 5 core needle samples obtained from a resected hereditary papillary renal carcinoma, but the levels of pMET species were near the assay lower limit of quantitation.

Conclusions: These validated immunoassays for pharmacodynamic biomarkers of MET signaling are suitable for studying MET responses in amplified cancers as well as compensatory responses to VEGFR blockade. Incorporating pharmacodynamic biomarker studies into clinical trials of MET inhibitors could provide critical proof-of-mechanism and proof-of-concept for the field.

Keywords

MET immunoassay; pharmacodynamic assays; MET inhibitor; translational biomarker; preclinical model

INTRODUCTION

The receptor tyrosine kinase (RTK) MET (MET proto-oncogene, receptor tyrosine kinase; hepatocyte growth factor receptor [HGFR]) is an important drug target because of its roles in cancer progression, metastasis, and acquired resistance to epidermal growth factor receptor (EGFR) inhibitors (1, 2). Aberrant MET signaling can occur through ligand-dependent as well as ligand-independent mechanisms (3). Consistent with multiple mechanisms of MET dysregulation, there are multiple therapeutic strategies to target MET, including HGF or MET neutralizing antibodies, decoy receptors, small-molecule tyrosine kinase inhibitors (TKIs), and allosteric inhibitors of MET activation (4-7). Drugs from each mechanistic class are currently under clinical investigation, both as single agents and in combination with other treatments (8-11). Many of these clinical trials require patient selection based on immunohistochemical and/or gene copy number assessment of MET (11, 12). However, these diagnostic assays cannot provide quantitative pharmacodynamic (PD) information (i.e., magnitude and duration of target modulation) to guide clinical development, nor can they distinguish between phosphorylated epitopes of full-length MET and its degradation products (13).

MET receptor activity is regulated by phosphorylation of a number of sites including Y1234 and Y1235 in the activation loop, which are crucial for regulation of kinase activity; the carboxy-terminal Y1349 and Y1356 in the multifunctional docking site required to recruit cytoplasmic signal transducers and adaptors; and S975 and Y1003 in the juxta-membrane region, phosphorylation of which causes MET ubiquitylation and degradation (5, 8, 14, 15). Based on this understanding of MET signaling, we designed MET immunoassays to measure full-length, transmembrane MET protein and three key phosphospecies involved in its signal transduction: pY1234/1235-MET, pY1235-MET, and pY1356-MET. These assays were designed for measurement of wild-type MET, because mutations account for only 10%-30% of all cancer subtypes where MET acts as a driver (compilation at http://

www.vai.org/Met/Index.aspx) (16). After validating the immunoassays and specimen collection and processing methods in preclinical models, the possible clinical suitability of the immunoassays for studying MET in diseases without gene amplification was evaluated in a case of MET-driven hereditary papillary renal cell carcinoma (HPRC).

MATERIALS AND METHODS

Reagents.

Purchased antibodies were qualified for use, including antigen affinity purified goat polyclonal anti-human MET extracellular domain (catalog number AF276, R&D Systems); mouse monoclonal anti-full-length MET (clone Met4, Van Andel Research Institute); mouse monoclonal anti-C-terminal MET (clone L41G3) and rabbit monoclonal anti-pY1234/pY1235-MET (clone D26, Cell Signaling Technologies, Inc.). Two rabbit monoclonal antibodies (mAbs) specific to pY1235-MET (clone 23111) and pY1356-MET (clone 7334) were developed under contract with Epitomics Inc. using phosphorylated peptide antigens corresponding to amino acid sequences surrounding these tyrosine residues (Supplemental Materials). Recombinant MET (rMET) calibrator protein was produced in HEK293 cells (Supplemental Materials). Antibodies were biotinylated using Sulfo-NHS-LC-biotin (Thermo-Fisher Scientific). Details of commercially available key assay reagents are described in SOP341203 and SOP341206, available at http://dctd.cancer.gov/ResearchResources/ResearchResources-biomarkers.htm.

Animal models and drug administration.

Athymic nude mice (*nu/nu* NCr; Animal Production Program, NCI-Frederick) were implanted with the human cancer cell lines U87 (glioblastoma); A549 (lung carcinoma); MDA-MB-231 (breast carcinoma); HT-29 (colon carcinoma); or with GTL-16, MKN45, or SNU5 (all gastric carcinomas, MET-amplified) as described (17). All cell lines were obtained from the Division of Cancer Treatment and Diagnosis Repository, NCI-Frederick and authenticated using AmpFLSTR Identifiler (Applied Biosystems).

MET inhibitors PHA665752 (NSC 748798-T), PF02341066 (NSC 749769-Y, crizotinib), and tivantinib (NSC 758242); VEGFR inhibitor pazopanib (NSC 737754); and multikinase inhibitor sorafenib (NSC 747971, lot #747971-U/3) were provided by the Developmental Therapeutics Program, National Cancer Institute (NCI). Purity was established by proton-carbon NMR, HPLC, and mass spectrometry. Sorafenib was dissolved in DMSO for in vitro studies. PF02341066 and pazopanib were administered by oral gavage in a saline vehicle and PHA665752 by intraperitoneal (IP) injections in a vehicle composed of 10% DMSO in saline. Tivantinib was administered orally in a PEG 400:20% vitamin E tocopheryl polyethylene glycol succinate solution (60:40) vehicle.

The NCI Animal Production Program, NCI-Frederick, is accredited by the Association for Assessment and Accreditation of Laboratory Animal Care International and follows Public Health Service policy on the humane care and use of laboratory animals. All studies were conducted according to approved NIH Animal Care and Use Committee protocols.

Xenograft biopsy and tumor quarter collection and extract preparation.

Specimen collection and handling conditions were adaptations of those achievable in past NCI clinical trials (18, 19). Briefly, 18-gauge Temno Trucut needle biopsies were immediately flash frozen in O-ring-sealed, conical-bottomed, screw-cap, 1.5-mL Sarstedt cryovials. Tubes were sealed, returned to liquid nitrogen, and stored at −80°C until use. Whole xenograft tumors were collected on the same schedule as tumor biopsies by standard dissection methods and cut into 2 to 4 equal pieces with fine-point scissors before flash-freezing. All preclinical samples were frozen within 2 min of excision.

Tissue samples were processed by adding ice-cold Cell Extraction Buffer (Invitrogen) and supplemented with PhosSTOP (Roche) and protease inhibitor tablets (Roche) to the frozen tissue (0.35 mL buffer/biopsy and 0.75 mL buffer/tumor quarter). Tissue was immediately homogenized with a PRO200 homogenizer with a Multi-Gen adaptor (Pro Scientific) and a 5 mm generator at the maximum setting for 10 sec at 2°C to 8°C. The extract was vortexed and homogenization was repeated. Extracts were incubated at 2°C to 8°C for 60 min with orbital shaking, and clarified by centrifugation at 12,000×*g* for 5 min at 2°C to 8°C. Cleared supernatant was aspirated and aliquoted. Total protein was measured by Bradford protein assay procedure (Bio-Rad).

Determination of mouse content of human tumor xenografts.

Mice were inoculated bilaterally with human tumor line cells (1×10^7) and tumor growth monitored daily. One cohort of mice was grouped when tumors reached 100, 200, 400, 500, 800, 1000, 1500, or 2000 mg; the mean tumor size for each weight-bin was determined, and the tumors removed for analysis. A second cohort was euthanized 10, 14, 18, 22, 26, and 30 days post-implantation, irrespective of tumor size, and retrospectively grouped into 100, 200, 400, and 600 mg weight-bins. DNA from one tumor quarter from each animal was analyzed for mouse and human DNA content (20).

Xenograft ischemia study.

SNU5 tumor xenografts were staged to ~200 mg ($n = 5$/group). Needle biopsies were collected under anesthesia and immediately flash-frozen as controls. Tumors were excised and quarters transferred to sterile normal saline maintained at 25°C ± 3°C (cold ischemia) or 37°C (warm ischemia) for 1, 2, 3, 4, 5, 8, 10, 15, 30, or 60 min in temperature-controlled saline before being flash frozen. All flash-frozen samples were stored at −80°C, and lysates were processed within 2 wk of collection.

Fit-for-purpose MET inhibitor studies.

Fit-for-purpose studies result in validated PD assays and provide drug mechanism of action information. To demonstrate assay fit-for-purpose in preclinical models, mice bearing GTL-16 and SNU5 xenografts were randomized when tumors reached 200 ± 25 mm^3 in size and dosed daily for 8-10 days with vehicle, oral PF02341066 (6.25, 12.5 or 25 mg/kg), or IP PHA665752 (25 or 50 mg/kg). In a separate study, mice with SNU5 xenografts were staged to 200 mm^3 and treated for 8 days with vehicle (daily), pazopanib (100 mg/kg daily), tivantinib (200 mg/kg daily), or combinations of pazopanib (daily) with 2 dose levels of tivantinib (200 mg/kg daily or 200 mg/kg twice daily). Extracts of core needle biopsies

collected 4 h after tivantinib administration on Day 8 were analyzed for MET, pMET, and hypoxia inducible factor 1, alpha subunit (HIF-1α) (21).

Core needle biopsies of HPRC tumor.

Multiple 18-gauge needle biopsies were collected from a surgically-resected tumor from a patient with HPRC (Urologic Oncology Branch, NCI) within 2 min of resection and immediately flash frozen. The patient gave written informed consent for study inclusion and was enrolled in an NCI Institutional Review Board-approved protocol. Study design and conduct complied with all applicable regulations, guidances, and local policies.

MET immunoassay procedure.

The full-length MET immunoassay measures the total levels of full-length MET in tumor tissue samples, irrespective of phosphorylation status. An affinity-purified goat polyclonal antibody against human MET extracellular domain (catalog number AF276) was used to coat 8-well NUNC Maxisorp strips overnight at 2°C to 8°C with 1 μg/mL buffer (0.1 M sodium carbonate/bicarbonate buffer pH 9.6, 100 μL/well). Wells were blocked for 2 h with 1× PBS, 0.5% mannitol, 0.2% glycine, and 0.2% BSA, and strips were assembled on 96-well plate frames, freeze-dried, and sealed in desiccated pouches (6-month stability). For the immunoassay, 100 μL each of purified rMET calibrator, controls, and tumor lysates (at protein concentrations of 10-50 μg/mL) prepared in assay buffer (1× PBS/Casein [BioFx] containing PhosSTOP, protease inhibitors and 0.1% Triton X-100 [Roche]) were added to the AF276-coated wells. The rMET assay calibrator was prepared for the dynamic range of the assay. Plates were incubated at ambient temperature (25°C ± 3°C) on an orbital shaker (600 rpm) 1 h to capture MET. After three washes with assay buffer,100 μL/well 200 ng/mL biotin-conjugated mouse monoclonal MET antibody (clone L41G3) was added to the plates and incubated 1 h at 25°C ± 3°C, followed by a second wash and the addition of 100 μL/well 200 ng/mL streptavidin poly-HRP conjugate (Pierce). After 30-min incubation with the HRP-conjugate, plates were washed 4 times and 100 μL SuperSignal ELISA Pico Chemiluminescent Substrate (Pierce) was added to each well. Plates were read within 10 min using an Infinite 200 Microplate ELISA reader (Tecan, USA). MET immunoassay calibration curves were analyzed on GraphPad Prism and unknown values were calculated using 4-parameter curve fitting.

Three different pMET immunoassays were developed for the PD studies: pY1234/1235-, pY1235-, and pY1356-MET (Supplemental Material). The pMET immunoassay procedures were similar to the full-length MET immunoassay except that rabbit mAbs specific to pY1234/1235-MET (clone D26, Cell Signaling Technologies), pY1235-MET (clone 23111), or pY1356-MET (clone 7334) were conjugated to biotin and used as reporter antibodies for the immunoassay. The pMET assay calibrators were prepared for the dynamic range of each assay. Assay control samples were prepared by combining GTL-16, SNU5, A549, MKN45, or U87 xenograft tumor lysates to achieve low, medium, and high MET concentrations at 10 to 50 μg/mL total protein concentrations.

MET immunofluorescence analysis.

HT-29, GTL-16 and A549 cancer cell lines were treated with DMSO vehicle (0.1% w/v), 100 nM PF02341066, or 100 nM sorafenib for 24 h at 37°C. Cells were fixed in 10% neutral-buffered formalin (Sigma-Aldrich) for 24 h, pelleted, and then embedded in paraffin. After 5-μm sectioning, antigen retrieval with Bond Epitope Retrieval Solution 2 (at 100°C for 10 min) and immunofluorescent staining were performed on the Bond-max Autostainer (Leica Biosystems). For antigen detection, 10 μg/mL primary antibody (anti-pY1235–MET, clone 23111) was followed by 10 μg/mL goat anti-rabbit AF488 (Life Technologies). Immunofluorescence microscopy was performed on core needle biopsies of a resected a human HPRC tumor stained with 5 μg/mL anti-full-length MET (clone Met4) followed by 10 μg/mL anti-mouse AF660 (Life Technologies). Image acquisition and analysis were performed on a wide-field fluorescent, confocal microscope (Nikon 90i, Andor Camera, NIS Elements Software).

Statistical analyses.

Regression analysis and descriptive statistics including means, standard deviations, coefficients of variation (CV), 1-way ANOVA analyses, and Student's t-tests were conducted with Microsoft Excel and GraphPad Prism (v3.04). The 95% confidence interval was significant at $\alpha = 0.05$ for a two-sided t-test.

RESULTS

Design and development of sandwich immunoassays for measuring Key phosphoMET species.

Tyrosines 1234, 1235, and 1356 mediate MET signal transduction via phosphorylation; so many MET-targeted agents are designed to reduce MET phosphorylation at one or more of these sites. To study the PD of such drugs, a sandwich immunoassay was designed to capture MET via its extracellular domain and then probe the captured MET for a particular phospho-epitope (pY1234/1235, pY1235 or pY1356) using specific monoclonal antibodies (Figure 1A). The capture antibody essentially did not cross-react with recombinant extracellular domains of the two most likely cross-reactive human tyrosine kinases, RON (macrophage stimulating 1 receptor; MST1R) and EGFR. At 10-fold excess concentration (4-400 pM) over rMET (0.4-40 pM), cross-reactivity with RON was < 5% and EGFR cross-reactivity was not detectable (data not shown). The pY1235-MET species was measured using a new rabbit mAb (clone 23111) that recognizes the pY1235 epitope independent of Y1234 phosphorylation status, and its high specificity was demonstrated by Western blot analysis using synthetic peptides, rMET, cell lysates, and mouse tissues (Figures S1A and S1D). Unlike the specificity of D26 antibody for the dual phosphorylated pY1234/pY1235 epitope, the mAb produced by clone 23111 showed no cross-reactivity with the cytoplasmic domain of RON or with this MET epitope when phosphorylated only at Y1234 or when tyrosine 1235 was replaced by aspartic acid (Figures S1A and S1B). It stained the plasma membrane of MET-expressing cell lines in an HGF-dependent manner that was sensitive to MET inhibitors, but not sorafenib (Figure 1B). A new rabbit mAb recognizing the pY1356 epitope of MET (clone 7334) was also generated for use in the immunoassay (Figure S1C, S1D).

Analytical validation of the sandwich immunoassays

Using full-length, purified rMET as calibrator, the dynamic ranges of the calibration curves for each assay were established: 0.3-40 pM for full-length and pY1234/1235-MET assays and 3.125-200 pM for the pY1235- and pY1356-MET assays (Figure 1C). Assay sensitivities were 1.5, 1.5, 7.8, and 15.6 fmol/μg protein, respectively, and the assays did not significantly cross-react with mouse MET species (Supplemental Materials).

The MET immunoassays were subjected to a rigorous validation protocol for analytical performance using clinically relevant tumor sampling procedures (core needle biopsy of tumors in mice) and specimen preparation procedures (Supplemental Materials). Dilution linearity studies showed that tumor extracts could be diluted up to 8-fold without affecting assay performance (Table S1). Spike-recovery experiments of rMET in xenograft extracts established immunoassay accuracy. Recovery ranged from 78%-116% for full-length MET, pY1234/1235-MET, and pY1235-MET assays, and 86% ± 29% for pY1356-MET (mean ± SD; Table S1). Intra-plate ($n = 20$) and inter-day ($n = 5$) variation were evaluated using three xenograft tumor extracts assayed at minimum of five different days by two operators; intra-assay CV was < 10% and interassay CV was < 14% (Table S1). After reducing the procedures and operating parameters of the validated assay to SOPs, assay robustness was formally demonstrated by SOP-driven assay transfer from the development to the clinical testing laboratory as previously described (18, 22).

The validated assay was capable of quantifying full-length MET in extracts of GTL-16, A549, MDA-MB-231, and U87 xenograft tumors over a wide range of protein loads per well (Figure 1D). Full-length MET was detected over a range of 0.05-1.79 fmol/μg protein, and as expected the MET-amplified model (GTL-16) contained the highest levels (1.31-1.79 fmol/μg protein). A least significant change (LSC) calculation, which combines both technical variation of the assay and biological variation of the biomarker (determined by analyzing multiple quadrants of xenografted SNU5 tumors), established a 45% change as the minimal effect level required to demonstrate a drug effect (Supplemental Materials).

Biopsy handling to control preanalytical variables

Preanalytical variables (specimen handling, shipping, and storage procedures) can have a significant impact on the reliability of biomarker measurements in the laboratory, and phosphoproteins involved in dynamic responses of signaling pathways are notoriously labile during specimen collection due to ischemia and other factors (23-25). The stability of full-length MET and its phosphospecies was characterized in biopsies of SNU5 xenografts subjected to increasing ischemia time, which was defined as the total time needed for core needle biopsy sampling, specimen handling, and flash freezing. MET levels in core needle biopsy samples frozen immediately after collection from anesthetized animals (defined as the zero time point) were set as baseline (100%). Both pY1235- and pY1356-MET levels decreased by >60% during 15 min of cold ischemia (25°C ± 3°C), and continued decreasing over the next 15 min ($P < 0.05$; Figure 2A). During 15 min of warm ischemia (37°C), both pY1235- and pY1356-MET levels decreased by >80% ($P < 0.05$; Figure 2B). The pY1234/p1235-MET species exhibited similar degradation under these conditions (data not shown).

In contrast, full-length MET levels were relatively stable for up to 60 min of cold ischemia, but decreased significantly at 37°C (Figure 2A, 2B).

A follow-up study evaluated the stabilities of pMET and full-length MET during 8 min of cold ischemia. After just 3 min of cold ischemia, pY1234/1235-MET levels decreased by >50% ($P < 0.05$; Figure 2C). Based on Western blot results, loss of full-length pY1235-MET signal during cold ischemia was predominantly due to loss of the pY1235-MET epitope, plus a small amount of degradation of full-length MET (the appearance of N- and C-terminal fragments, Figure 2D). Stabilities of the pY1234/1235-MET and pY1356-MET analytes were similar (data not shown). Therefore, core needle biopsies frozen within 2 min of collection will yield valid pMET assay results.

Pharmacodynamics of MET RTK inhibitors in gastric carcinoma xenograft models

Mice with GTL-16 tumor xenografts, a MET-amplified model, were treated daily with the MET inhibitors, PHA665752 or PF02341066, and sampled at clinically relevant time points (4 or 24 h) after drug administration. The 25 and 50 mg/kg/day dose levels of PHA665752 slowed the growth of GTL-16 xenograft tumors and achieved tumor stasis after 8-10 days of treatment (Figure 3A, Study Days 17-19). Four h after the first dose there was a dose-dependent reduction in the pY1235-MET:MET ratio of 62% and 80%, respectively (Figure 3B), effect sizes that exceeded the LSC threshold of 45%. Over the next 20 h, the pY1235-MET:MET ratio partially to fully recovered, depending upon dosage. Additional daily doses of 50 mg/kg PHA665752 significantly decreased the pY1235-MET:MET ratio, while the 25 mg/kg dose produced inconsistent changes (Figure 3B). The ratio of pY1356-MET:MET also declined after the first dose, although it recovered to normal levels within 20 h (Figure S3A). Therefore, the tumor stasis observed with this agent and dosage regimen was associated with intervals of modest reductions in the pY1235 and pY1356 targets followed by target recovery. The absolute level of full-length MET also decreased by 40%-50% within 10 days of treatment with either vehicle or drug (Figure S3B).

As previously reported (10), treatment of GTL-16 xenografts with daily oral PF02341066 at the 25 mg/kg dose level achieved stasis of GTL-16 xenografts by the seventh day of treatment (Figure 3C; Study Day 11). Only this dose level reduced the pY1235-MET:MET ratio (by 65%) 4 h after treatment, and this ratio recovered completely during the next 20 h (Figure 3D). Additional daily doses of PF02341066 further reduced the pY1235-MET:MET ratio, so molecular target control 4 h after each dose was achievable throughout the daily treatment period. The SNU5 model exhibited a similar dose-dependent PD response to PF02341066, and again pointed to greater PD responsiveness of pY1235 than pY1356 following TKI therapy (Figure S4).

A second study of GTL-16 xenografts treated daily with PF02341066, but with denser tumor sampling to more fully characterize the PD response, confirmed that only the 25 mg/kg/day dose level achieved a molecular target response after the first dose. However, there was a cumulative, dose-dependent PD effect on the pY1235-MET:MET ratio such that by Day 4, both the 25 and 12.5 mg/kg dose levels produced PD responses 4 h and 12 h after drug administration, although only the higher dose maintained this PD response for the entire 24-hour dosing interval (Figure 4A). The pY1356-MET:MET ratio decreased after 4 and 12 h

but fully recovered by 24 h at both dose levels (Figure 4B). Again, full-length MET levels decreased by 40%-50% by treatment day 10 in both drug- and vehicle-treated groups (Figure 4C).

This preclinical modeling suggest that greater control of MET signaling than the intermittent 80% reduction in the pMET:MET ratio observed here will be needed to achieve regressions of MET-amplified tumor models. These data also indicate the importance of using the more consistent pMET:MET ratio instead of absolute levels of particular pMET species as PD endpoints, at least in preclinical models where mouse cell infiltration of human tumor xenografts over time diluted the absolute level of human MET per microgram extracted protein (Figure S5).

Fit-for-purpose modeling of the first-in-human application of the assay

The first clinical application of the validated assay is assessment of tumor PD response during a phase 1 clinical trial of the VEGFR/PDGFR inhibitor pazopanib alone and in combination with the MET inhibitor tivantinib (ClinicalTrials.gov NCT01468922). The trial is testing two hypotheses: (i) MET will be upregulated as part of a compensatory response to VEGFR/PDGFR inhibition by pazopanib, and (ii) tivantinib will blunt that upregulation by inducing degradation of total MET (26). To model this trial, mice bearing SNU5 xenografts were treated with vehicle or the drugs individually or in combination and the tumors were sampled on day 8 using 18-gauge biopsy needles to replicate the sampling planned for the clinical trial. Neither single-agent pazopanib nor tivantinib affected full-length MET levels (Figure 5A). However, treatment with pazopanib, but not tivantinib, increased both pY1235-MET:MET and pY1356-MET:MET ratios compared to vehicle (Figure 5B, C). Twice daily tivantinib (200 mg/kg BID) combined with pazopanib returned the pMET:MET ratios to vehicle-treated levels, whereas daily tivantinib treatment (200 mg/kg QD) caused an intermediate effect (Figure 5B, C). To determine whether the underlying changes in MET levels were associated with hypoxia induced by VEGFR/PDGFR inhibition, HIF-1α levels were measured using a validated HIF-1α immunoassay (21). Pazopanib-induced increases in pMET:MET ratios were accompanied by a 46% increase in HIF-1α levels ($p < 0.05$), whereas the addition of tivantinib returned HIF-1α to vehicle-treated levels (Figure 5D).

MET and pMET levels in clinical cancer without MET amplification: HPRC

The baseline levels of MET and pMET in human tumor models without MET amplification (Figure 1D) are low, lying near the assay lower limit of quantitation; therefore drug-induced decreases in pMET:MET ratios cannot be quantified in these models. To address the question whether or not MET and pMET levels in preclinical models and in clinical cancer without substantial *MET* amplification are similar, we evaluated core needle biopsies of five regions of a resected HPRC tumor harboring a germ line *MET* mutation (H1112R). HPRC is characterized by germline trisomy of chromosome 7, frequent expression of two copies of mutated *MET* and one copy of wild-type *MET* (27, 28), and decreased activation threshold of the kinase activity and enhanced transforming activity (15), so HPRC was a non-amplified disease in which pMET quantitation seemed likely. As expected, full-length MET levels ranged from 0.073 to 0.368 fmol/μg protein (Table S2), similar to nonamplified models. However, pY1234/1235-MET was measurable in only two of five cores (0.037 and

0.041 fmol/μg), and neither pY1235-MET nor pY1356-MET were detectable in any core specimen.

Immunofluorescence staining of sections of the HPRC cores with the capture antibody from the immunoassay (AF276, anti-MET extracellular domain) confirmed the presence of MET in the HPRC cells and localized it primarily to the plasma membrane (Figure 6A). Western blotting revealed that the undetectable level of pY1235-MET in the immunoassay was due in large part to the association of the epitope with a truncated C-terminal 50 kDa MET fragment (Figure 6B), which is too small to contain the N-terminal domain required for capturing full-length MET in the validated sandwich immunoassay. A small amount of full-length MET containing the pY1235 epitope was detectable by Western blotting, but detection required loading the gel lane with 25-50 μg total protein, which exceeds the amount of protein that can be used in the immunoassay while maintaining assay linearity (Figure 1D). Interestingly, the antibody against pY1234/1235-MET (clone D26) recognized mainly full-length MET (Figure 6B), which is why it was detectable in the immunoassay.

DISCUSSION

Biochemical signaling from activated MET drives both proliferation and migration of malignant cells (1, 2), and MET can be activated not only by conventional ligand binding of paracrine and autocrine HGF but also by several ligand-independent mechanisms. Transphosphorylation of Y1235 in the kinase domain initiates signaling, and subsequent phosphorylation of Y1349 and Y1356 in the SH2 binding motif transduces signaling, with phosphorylation of Y1356 critical for growth factor receptor bound protein 2 docking that may link MET to the RAS pathway (29, 30), analogous to EGFR signaling. Several pharmacological classes of MET inhibitors target these key phosphorylation events, so the extent of phosphorylation of the critical tyrosine residues should be a highly informative PD biomarker of molecular drug action. Importantly, we demonstrated that the phosphorylation status of the key tyrosine residues in full-length ligand-responsive MET is quantifiable using a dual-epitope sandwich-immunoassay platform with newly generated monoclonal antibodies specific for pY1356 and for pY1235 (independent of phosphorylation status of the adjacent Y1234 residue) that will be made available to the research community via the Developmental Studies Hybridoma Bank (http://dshb.biology.uiowa.edu/). Also, to obtain valid assay results, cold ischemia time must be limited to 2 min to preserve the phosphorylated analytes. For preclinical PD studies in xenograft models, a human pMET:MET ratio normalizes pMET to total MET and mitigates the confounding effect of mouse cell infiltration as tumors grow (20).

Daily dosage regimens of two MET TKIs achieved tumor control and PD responses in GTL-16 and SNU5 human tumor xenograft models of poorly differentiated gastric carcinoma driven by MET-amplification (31, 32). Tumor control of GTL-16 with PHA665752, a highly selective, ATP-competitive inhibitor of MET RTK activity (33), was associated with a 60-80% reduction in the pY1235-MET:MET ratio 4 h after the first dose, but the ratio fully recovered by 24 h and was less responsive to subsequent days of therapy. Treating GTL-16 with PF02341066, a potent, orally bioavailable, ATP-competitive inhibitor of MET catalytic activity (34), achieved tumor control at the only dose level that elicited a

PD response (a consistent 65-90% reduction in the pY1235-MET:MET ratio throughout the 24-hour dosing interval). The pY1356-MET:MET ratio was consistently less responsive to drug therapy than the pY1235-MET:MET ratio in both tumor models and with both MET TKIs, suggesting GRB2 signaling is more difficult to inhibit than MET kinase activity.

Importantly, 60-90% reductions in the pY1235-MET:MET ratio were associated only with tumor stasis, but not regression. Therefore, a greater than commonly seen MET PD response, i.e., the magnitude and/or duration of pY1235-MET inhibition, or the addition of pY1356-MET inhibition (also linked to tumor regression) (35) must be needed to induce tumor regression in MET-amplified models. Clinical benefit from MET-directed therapy has been limited to patients with high baseline MET expression (36-39), but these assessments were made without a validated PD biomarker for activated MET or knowledge of the effect of warm ischemia on full-length MET degradation. Therefore, the trials to date unfortunately represent missed opportunities to understand clinical PD responses elicited by current MET inhibitors that could guide their future clinical development (40). The newly developed and validated assays described here are suitable for defining the PD response associated with tumor regression both in preclinical models and human patients with MET amplified cancers. The analytical performance of the assays is sufficient for conducting small, fast phase 0 clinical trials of various dosage regimens of investigational MET inhibitors to discover how to maintain over 90% target suppression during dosing intervals (41, 42). From our error modeling, considering both biological variability and assay precision, clinical PD study designs based on longitudinal patient sampling should require decreases in pMET:MET ratios of at least 45% (the LSC value) to attribute them to drug effect,

In addition to MET amplification with its relatively high baseline pMET:MET ratios, assay fitness-for-purpose was also demonstrated in a MET-induction setting during compensatory responses to tumor hypoxia. Induction of MET signaling converts a tumor from low to measurably high MET and pMET levels, which become targets of MET TKI therapy. We found that pharmacological targeting of tumor vasculature in SNU5 xenografts with pazopanib, a multi-kinase inhibitor, induced the hypoxia biomarker Hif-1α and increased pY1235-MET:MET and pY1356-MET:MET ratios. Although twice daily treatment with tivantinib, an allosteric inhibitor of MET (6, 7, 26) with some effects on microtubules (43-45), did not reduce baseline MET or pMET levels, it nevertheless blocked pazopanib-induced HIF-1α MET signaling. Several molecular mechanisms could explain why tivantinib blocked pMET increases induced by pazopanib, including blocking the microtubule dependent co-clustering of MET and VEGFR2 or prolonging PTP1B (protein tyrosine phosphatase, non-receptor type 1) inhibition of MET (43, 44, 46). Clinical trials of MET/VEGF inhibitor combinations [pazopanib/tivantinib (NCT01468922) and bevacizumab/tivantinib (NCT01749384)] provide an opportunity for correlative PD studies to determine if this compensatory mechanism operates in clinical cancers, and the preclinical modeling of one of these trials demonstrated that the validated pMET immunoassay is a suitable tool for these studies.

This newly developed and validated immunoassay for PD biomarkers of MET molecular response is a robust tool for understanding and optimizing pharmacological control of both amplified and induced MET signaling, and it is ready for training-based transfer to the

research community by the NCI (http://dctd.cancer.gov/ResearchResources/ResearchResources-biomarkers.htm). Phosphorylation of Y1235 is the proposed first step of MET signaling upon ligand binding, and the specificity of the new mAb for phosphorylated Y1235 independent of the phosphorylation status of the adjacent Y1234 residue will be useful for teasing apart the role of these neighboring tyrosines during initiation of MET signaling and molecular response to MET TKIs. Importantly, the anti-pY1235 mAb we generated (clone 23111) exhibited much greater specificity than the anti-pY1234/1235 mAb (clone D26), which even recognized a recombinant GST-MET protein harboring a Y1235D substitution. Our studies found that PD responses of the pY1235 and pY1234/1235 biomarkers did not always correspond. Furthermore, both pY1235 and pY1234/1235 epitopes were identified in full-length MET extracted from an HPRC tissue sample, while the pY1235 epitope was mostly present in a 50 kDa MET fragment. Similarly complex phosphorylation profiles have been found in non-small cell lung cancer in which only 25% of MET+ cases were also positive for pY1234/1235-MET (47). The pY1235-specific antibody could be a key reagent in a new diagnostic test for selecting the right patients to receive MET-targeted therapies because it substitutes the phosphorylated MET kinase domain (48) in place of elevated MET, mRNA, gene copy number, co-localized proteins, or multiply phosphorylated epitopes (49, 50). However, unlike the validated immunoassay, cross-reactivity to MET fragments with undefined biological significance (27) will confound the reported immunohistochemical tests of MET signaling (26, 37, 51-53).

Supplementary Material

Refer to Web version on PubMed Central for supplementary material.

ACKNOWLEDGEMENTS

The authors would like to thank Drs. Andrea Regier Voth, Leidos Biomedical Research, Inc. and Joseph Shaw, Kelly Services, for knowledgeable and skilled medical writing support in the preparation of this manuscript.

Financial Support: This project has been funded in whole or in part with federal funds from the National Cancer Institute, National Institutes of Health, under Contract No. HHSN261200800001E. The content of this publication does not necessarily reflect the views or policies of the Department of Health and Human Services, nor does mention of trade names, commercial products, or organizations imply endorsement by the U.S. Government.

REFERENCES

1. Engelman JA, Zejnullahu K, Mitsudomi T, Song Y, Hyland C, Park JO, et al. MET amplification leads to gefitinib resistance in lung cancer by activating ERBB3 signaling. Science 2007;316:1039–43. [PubMed: 17463250]
2. Guo A, Villen J, Kornhauser J, Lee KA, Stokes MP, Rikova K, et al. Signaling networks assembled by oncogenic EGFR and c-Met. Proc Natl Acad Sci U S A 2008;105:692–7. [PubMed: 18180459]
3. Brooks AN, Choi PS, de Waal L, Sharifnia T, Imielinski M, Saksena G, et al. A pan-cancer analysis of transcriptome changes associated with somatic mutations in U2AF1 reveals commonly altered splicing events. PLoS One 2014;9:e87361. [PubMed: 24498085]
4. Eder JP, Shapiro GI, Appleman LJ, Zhu AX, Miles D, Keer H, et al. A phase I study of foretinib, a multi-targeted inhibitor of c-Met and vascular endothelial growth factor receptor 2. Clin Cancer Res 2010;16:3507–16. [PubMed: 20472683]
5. Trusolino L, Bertotti A, Comoglio PM. MET signalling: principles and functions in development, organ regeneration and cancer. Nat Rev Mol Cell Biol 2010;11:834–48. [PubMed: 21102609]

6. Eathiraj S, Palma R, Hirschi M, Volckova E, Nakuci E, Castro J, et al. A novel mode of protein kinase inhibition exploiting hydrophobic motifs of autoinhibited kinases: discovery of ATP-independent inhibitors of fibroblast growth factor receptor. J Biol Chem 2011;286:20677–87. [PubMed: 21454610]
7. Eathiraj S, Palma R, Volckova E, Hirschi M, France DS, Ashwell MA, et al. Discovery of a novel mode of protein kinase inhibition characterized by the mechanism of inhibition of human mesenchymal-epithelial transition factor (c-Met) protein autophosphorylation by ARQ 197. J Biol Chem 2011;286:20666–76. [PubMed: 21454604]
8. Eder JP, Vande Woude GF, Boerner SA, LoRusso PM. Novel therapeutic inhibitors of the c-Met signaling pathway in cancer. Clin Cancer Res 2009;15:2207–14. [PubMed: 19318488]
9. Kurzrock R, Sherman SI, Ball DW, Forastiere AA, Cohen RB, Mehra R, et al. Activity of XL184 (Cabozantinib), an oral tyrosine kinase inhibitor, in patients with medullary thyroid cancer. J Clin Oncol 2011;29:2660–6. [PubMed: 21606412]
10. Rodig SJ, Shapiro GI. Crizotinib, a small-molecule dual inhibitor of the c-Met and ALK receptor tyrosine kinases. Curr Opin Investig Drugs 2010;11:1477–90.
11. Santoro A, Rimassa L, Borbath I, Daniele B, Salvagni S, Van Laethem JL, et al. Tivantinib for second-line treatment of advanced hepatocellular carcinoma: a randomised, placebo-controlled phase 2 study. Lancet Oncol 2013;14:55–63. [PubMed: 23182627]
12. Surati M, Patel P, Peterson A, Salgia R. Role of MetMAb (OA-5D5) in c-MET active lung malignancies. Expert Opin Biol Ther 2011;11:1655–62. [PubMed: 22047509]
13. Lefebvre J, Ancot F, Leroy C, Muharram G, Lemiere A, Tulasne D. Met degradation: more than one stone to shoot a receptor down. FASEB J 2012;26:1387–99. [PubMed: 22223753]
14. Zhu H, Naujokas MA, Fixman ED, Torossian K, Park M. Tyrosine 1356 in the carboxyl-terminal tail of the HGF/SF receptor is essential for the transduction of signals for cell motility and morphogenesis. J Biol Chem 1994;269:29943–8. [PubMed: 7961992]
15. Chiara F, Michieli P, Pugliese L, Comoglio PM. Mutations in the met oncogene unveil a "dual switch" mechanism controlling tyrosine kinase activity. J Biol Chem 2003;278:29352–8. [PubMed: 12746450]
16. Voortman J, Harada T, Chang RP, Killian JK, Suuriniemi M, Smith WI, et al. Detection and therapeutic implications of c-Met mutations in small cell lung cancer and neuroendocrine tumors. Curr Pharm Des 2013;19:833–40. [PubMed: 22973954]
17. Plowman J, Dykes D, Hollingshead M, Simpson-Herren L, Alley M. Human tumor xenograft models in NCI drug development In: Teicher B, editor. Anticancer drug development guide Preclinical screening, clinical trials, and approvaled. Totowa, NJ: Humana Press Inc; 1997 p. 101–25.
18. Pfister TD, Hollingshead M, Kinders RJ, Zhang Y, Evrard YA, Ji J, et al. Development and validation of an immunoassay for quantification of topoisomerase I in solid tumor tissues. PLoS One 2012;7:e50494. [PubMed: 23284638]
19. Kinders RJ, Hollingshead M, Khin S, Rubinstein L, Tomaszewski JE, Doroshow JH, et al. Preclinical modeling of a phase 0 clinical trial: qualification of a pharmacodynamic assay of poly (ADP-ribose) polymerase in tumor biopsies of mouse xenografts. Clin Cancer Res 2008;14:6877–85. [PubMed: 18980982]
20. Alcoser SY, Kimmel DJ, Borgel SD, Carter JP, Dougherty KM, Hollingshead MG. Real-time PCR-based assay to quantify the relative amount of human and mouse tissue present in tumor xenografts. BMC Biotechnol 2011;11:124. [PubMed: 22176647]
21. Park SR, Kinders RJ, Khin S, Hollingshead M, Parchment RE, Tomaszewski JE, et al. Validation and fitness testing of a quantitative immunoassay for HIF-1 alpha in biopsy specimens. Cancer Res 2012;Cancer Res 2012;72(8 Suppl):Abstract nr 3616:8.
22. Kinders RJ, Hollingshead M, Lawrence S, Ji J, Tabb B, Bonner WM, et al. Development of a validated immunofluorescence assay for gammaH2AX as a pharmacodynamic marker of topoisomerase I inhibitor activity. Clin Cancer Res 2010;16:5447–57. [PubMed: 20924131]
23. Baker AF, Dragovich T, Ihle NT, Williams R, Fenoglio-Preiser C, Powis G. Stability of phosphoprotein as a biological marker of tumor signaling. Clin Cancer Res 2005;11:4338–40. [PubMed: 15958615]

24. Neumeister VM, Parisi F, England AM, Siddiqui S, Anagnostou V, Zarrella E, et al. A tissue quality index: an intrinsic control for measurement of effects of preanalytical variables on FFPE tissue. Lab Invest 2014;94:467–74. [PubMed: 24535259]
25. Wolf C, Jarutat T, Vega Harring S, Haupt K, Babitzki G, Bader S, et al. Determination of phosphorylated proteins in tissue specimens requires high-quality samples collected under stringent conditions. Histopathology 2014;64:431–44. [PubMed: 24266863]
26. Yap TA, Olmos D, Brunetto AT, Tunariu N, Barriuso J, Riisnaes R, et al. Phase I trial of a selective c-MET inhibitor ARQ 197 incorporating proof of mechanism pharmacodynamic studies. J Clin Oncol 2011;29:1271–9. [PubMed: 21383285]
27. Zhuang Z, Park WS, Pack S, Schmidt L, Vortmeyer AO, Pak E, et al. Trisomy 7-harbouring non-random duplication of the mutant MET allele in hereditary papillary renal carcinomas. Nat Genet 1998;20:66–9. [PubMed: 9731534]
28. Schmidt L, Junker K, Weirich G, Glenn G, Choyke P, Lubensky I, et al. Two North American families with hereditary papillary renal carcinoma and identical novel mutations in the MET proto-oncogene. Cancer Res 1998;58:1719–22. [PubMed: 9563489]
29. Hartmann G, Weidner KM, Schwarz H, Birchmeier W. The motility signal of scatter factor/hepatocyte growth factor mediated through the receptor tyrosine kinase met requires intracellular action of Ras. J Biol Chem 1994;269:21936–9. [PubMed: 8071312]
30. Cepero V, Sierra JR, Corso S, Ghiso E, Casorzo L, Perera T, et al. MET and KRAS gene amplification mediates acquired resistance to MET tyrosine kinase inhibitors. Cancer Res 2010;70:7580–90. [PubMed: 20841479]
31. Rege-Cambrin G, Scaravaglio P, Carozzi F, Giordano S, Ponzetto C, Comoglio PM, et al. Karyotypic analysis of gastric carcinoma cell lines carrying an amplified c-met oncogene. Cancer Genet Cytogenet 1992;64:170–3. [PubMed: 1486568]
32. Park JG, Frucht H, LaRocca RV, Bliss DP Jr., Kurita Y, Chen TR, et al. Characteristics of cell lines established from human gastric carcinoma. Cancer Res 1990;50:2773–80. [PubMed: 2158397]
33. Christensen JG, Schreck R, Burrows J, Kuruganti P, Chan E, Le P, et al. A selective small molecule inhibitor of c-Met kinase inhibits c-Met-dependent phenotypes in vitro and exhibits cytoreductive antitumor activity in vivo. Cancer Res 2003;63:7345–55. [PubMed: 14612533]
34. Zou HY, Li Q, Lee JH, Arango ME, McDonnell SR, Yamazaki S, et al. An orally available small-molecule inhibitor of c-Met, PF-2341066, exhibits cytoreductive antitumor efficacy through antiproliferative and antiangiogenic mechanisms. Cancer Res 2007;67:4408–17. [PubMed: 17483355]
35. Rikova K, Guo A, Zeng Q, Possemato A, Yu J, Haack H, et al. Global survey of phosphotyrosine signaling identifies oncogenic kinases in lung cancer. Cell 2007;131:1190–203. [PubMed: 18083107]
36. Blumenschein GR Jr., Mills GB, Gonzalez-Angulo AM. Targeting the hepatocyte growth factor-cMET axis in cancer therapy. J Clin Oncol 2012;30:3287–96. [PubMed: 22869872]
37. Knudsen BS, Zhao P, Resau J, Cottingham S, Gherardi E, Xu E, et al. A novel multipurpose monoclonal antibody for evaluating human c-Met expression in preclinical and clinical settings. Appl Immunohistochem Mol Morphol 2009;17:57–67. [PubMed: 18815565]
38. Miyamoto M, Ojima H, Iwasaki M, Shimizu H, Kokubu A, Hiraoka N, et al. Prognostic significance of overexpression of c-Met oncoprotein in cholangiocarcinoma. Br J Cancer 2011;105:131–8. [PubMed: 21673683]
39. Sattler M, Reddy MM, Hasina R, Gangadhar T, Salgia R. The role of the c-Met pathway in lung cancer and the potential for targeted therapy. Ther Adv Med Oncol 2011;3:171–84. [PubMed: 21904579]
40. Garber K MET inhibitors start on road to recovery. Nat Rev Drug Discov 2014;13:563–5. [PubMed: 25082276]
41. Kummar S, Kinders R, Gutierrez ME, Rubinstein L, Parchment RE, Phillips LR, et al. Phase 0 clinical trial of the poly (ADP-ribose) polymerase inhibitor ABT-888 in patients with advanced malignancies. J Clin Oncol 2009;27:2705–11. [PubMed: 19364967]

42. Kummar S, Anderson L, Hill K, Majerova E, Allen D, Horneffer Y, et al. First-in-human phase 0 trial of oral 5-iodo-2-pyrimidinone-2'-deoxyribose in patients with advanced malignancies. Clin Cancer Res 2013;19:1852–7. [PubMed: 23403637]
43. Basilico C, Pennacchietti S, Vigna E, Chiriaco C, Arena S, Bardelli A, et al. Tivantinib (ARQ197) displays cytotoxic activity that is independent of its ability to bind MET. Clin Cancer Res 2013;19:2381–92. [PubMed: 23532890]
44. Katayama R, Aoyama A, Yamori T, Qi J, Oh-hara T, Song Y, et al. Cytotoxic activity of tivantinib (ARQ 197) is not due solely to c-MET inhibition. Cancer Res 2013;73:3087–96. [PubMed: 23598276]
45. Aoyama A, Katayama R, Oh-Hara T, Sato S, Okuno Y, Fujita N. Tivantinib (ARQ 197) exhibits antitumor activity by directly interacting with tubulin and overcomes ABC transporter-mediated drug resistance. Mol Cancer Ther 2014;13:2978–90. [PubMed: 25313010]
46. Lu KV, Chang JP, Parachoniak CA, Pandika MM, Aghi MK, Meyronet D, et al. VEGF inhibits tumor cell invasion and mesenchymal transition through a MET/VEGFR2 complex. Cancer Cell 2012;22:21–35. [PubMed: 22789536]
47. Tsuta K, Kozu Y, Mimae T, Yoshida A, Kohno T, Sekine I, et al. c-MET/phospho-MET protein expression and MET gene copy number in non-small cell lung carcinomas. J Thorac Oncol 2012;7:331–9. [PubMed: 22198430]
48. Furlan A, Kherrouche Z, Montagne R, Copin MC, Tulasne D. Thirty years of research on met receptor to move a biomarker from bench to bedside. Cancer Res 2014;74:6737–44. [PubMed: 25411347]
49. Scagliotti GV, Novello S, Schiller JH, Hirsh V, Sequist LV, Soria JC, et al. Rationale and design of MARQUEE: a phase III, randomized, double-blind study of tivantinib plus erlotinib versus placebo plus erlotinib in previously treated patients with locally advanced or metastatic, nonsquamous, non-small-cell lung cancer. Clin Lung Cancer 2012;13:391–5. [PubMed: 22440336]
50. Spigel DR, Edelman MJ, Mok T, O'Byrne K, Paz-Ares L, Yu W, et al. Treatment Rationale Study Design for the MetLung Trial: A Randomized, Double-Blind Phase III Study of Onartuzumab (MetMAb) in Combination With Erlotinib Versus Erlotinib Alone in Patients Who Have Received Standard Chemotherapy for Stage IIIB or IV Met-Positive Non-Small-Cell Lung Cancer. Clin Lung Cancer 2012;13:500–4. [PubMed: 23063071]
51. Iveson T, Donehower RC, Davidenko I, Tjulandin S, Deptala A, Harrison M, et al. Rilotumumab in combination with epirubicin, cisplatin, and capecitabine as first-line treatment for gastric or oesophagogastric junction adenocarcinoma: an open-label, dose de-escalation phase 1b study and a double-blind, randomised phase 2 study. Lancet Oncol 2014;15:1007–18. [PubMed: 24965569]
52. Spigel DR, Ervin TJ, Ramlau RA, Daniel DB, Goldschmidt JH Jr., Blumenschein GR Jr., et al. Randomized phase II trial of Onartuzumab in combination with erlotinib in patients with advanced non-small-cell lung cancer. J Clin Oncol 2013;31:4105–14. [PubMed: 24101053]
53. Gruver AM, Liu L, Vaillancourt P, Yan SC, Cook JD, Roseberry Baker JA, et al. Immunohistochemical application of a highly sensitive and specific murine monoclonal antibody recognising the extracellular domain of the human hepatocyte growth factor receptor (MET). Histopathology 2014;65:879–96. [PubMed: 25039923]

TRANSLATIONAL RELEVANCE

Inhibiting aberrant signaling of the receptor tyrosine kinase MET is a promising new therapeutic strategy for cancer treatment. Currently, several small molecule inhibitors and therapeutic antibodies targeting MET are in various stages of clinical development, but despite multiple clinical trials, clear evidence of target engagement and modulation in tumor tissue is lacking. We describe validated measurements of the phosphorylation status of critical tyrosine residues in MET for assessing its pharmacodynamic response to targeted tyrosine kinase inhibitors. The ability to monitor full-length MET and its key phosphospecies in tumor biopsies and pMET specifically in tumor xenografts will facilitate clinical studies that could link MET pharmacology to biology and clarify MET-based compensatory signaling in patients.

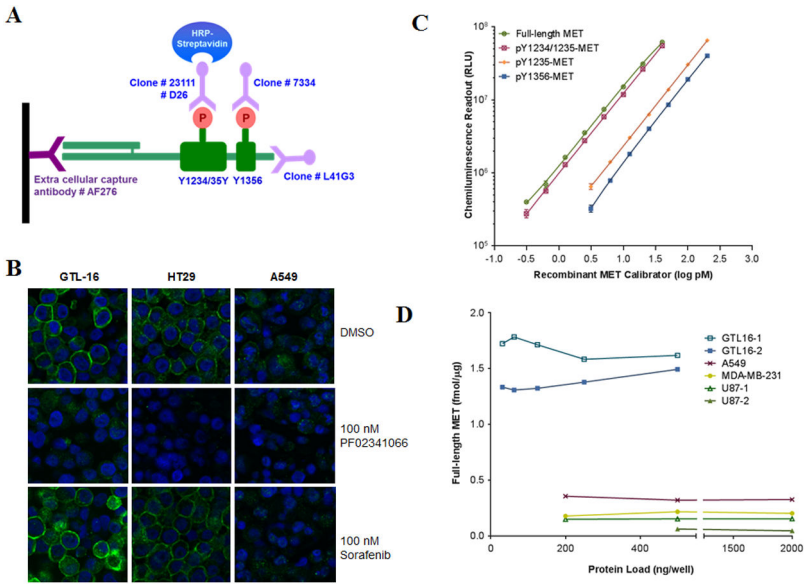

Figure 1. Development of immunoassays for full-length MET and its key phosphorylated species.

(A) Schematic of the MET immunoassays: a capture antibody (catalog number AF276) specific to the extracellular domain of MET binds and traps MET from tissue lysates, then four different reporter monoclonal antibodies (clone D26 to pY1234/1235, clone 23111 to pY1235, clone 7334 to pY1356 and clone L41G3 to the C-terminus) are used to detect phosphorylated and full-length MET. **(B)** Specificity of anti-pY1235-MET (clone 23111; developed in this study) is shown by immunofluorescence staining of formalin-fixed, paraffin-embedded GTL-16, HT29, and A549 cancer cells treated in vitro with 100 nM PF02341066 or 100 nM sorafenib for 4 h. **(C)** Representative calibration curves from the full-length MET (0.3-40 pM), pY1234/1235-MET (0.3-40 pM), pY1235-MET (1.5-200 pM), and pY1356-MET immunoassays (3.25-200 pM). The same rMET protein is used as a calibrator in all four immunoassays and levels have been converted to log pM. **(D)** MET levels in four different human cancer cell lines routinely used in MET preclinical xenograft studies; two separate GTL-16 and U87 xenograft samples were used. Cell lysates were diluted to 31.25-2000 ng/well in a 100 µL volume; MET levels were back-calculated to fmol/µg total loaded protein.

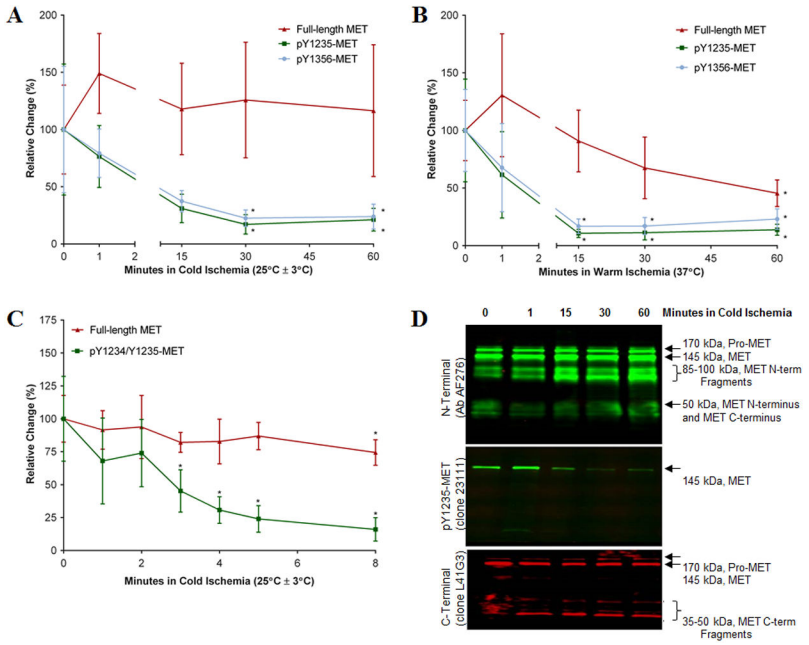

Figure 2. Stability of full-length MET and pMET in core needle biopsies of xenografted SNU5 tumors.

Core needle biopsies were incubated in saline solution for 0 (baseline, 100%), 1, 15, 30, or 60 min of **(A)** cold ischemia or **(B)** warm ischemia. **(C)** Follow-up study of stability of full-length and pY1234/1235-MET in core biopsies during 0, 1, 2, 3, 4, 5, and 8 min of cold ischemia. For all graphs, error bars are mean ± SD, $n = 4$-6; a single asterisk (*) denotes $P < 0.05$ from baseline by Student's t test. **(D)** Western blot of extracts of core biopsies after 0, 1, 15, 30 or 60 min of cold ischemia probed with the indicated antibodies.

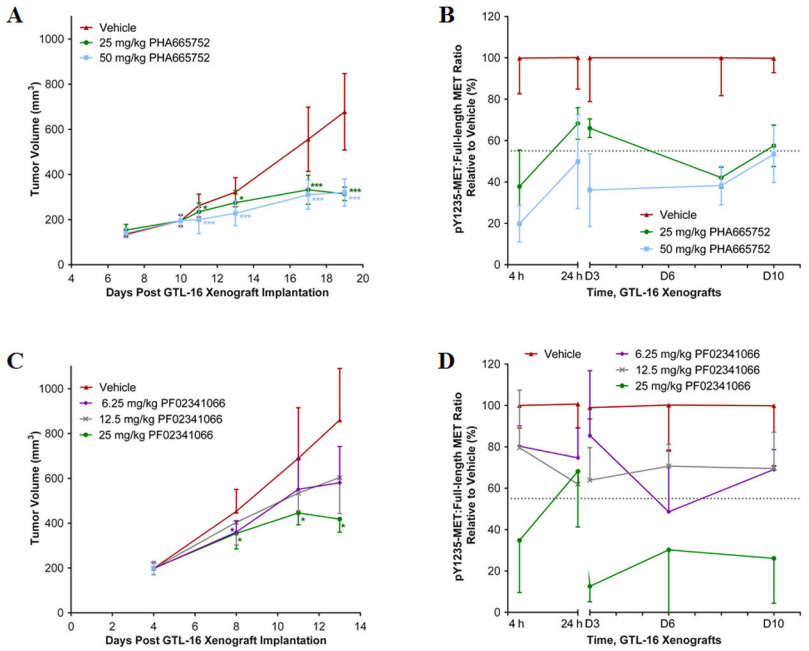

Figure 3. Reduction of GTL-16 tumor growth and MET phosphorylation by MET RTK inhibitors.

(A) Tumor volume of GTL-16 tumor xenografts in mice treated with PHA665752 at daily doses of 0, 25 and 50 mg/kg IP starting 10 days after implantation; n = 5-28 per dose per time point. **(B)** The intratumoral pY1235-MET:MET ratio during 10 days of daily treatment with PHA665752; n = 5-6 per dose per time point. Tumor samples were analyzed at 4 and 24 h after dose 1, and 4 h after dose 3 (D3), 8 (D8) and 10 (D10). **(C)** Tumor volume of GTL-16 xenografts in mice treated with PF02341066 at daily doses of 0, 6.25, 12.5, and 25 mg/kg PO starting at 4 days after implantation. Error bars are mean ± SD, groups n = 4-30 per dose per time point. **(D)** The pY1235-MET:MET ratio during 10 days of daily treatment with PF02341066. Tumor samples were analyzed at 4 and 24 h after dose 1 and 4 h after dose 3 (D3), 6 (D6) and 10 (D10). Mean ± SD, groups n = 2-6 per dose per time point. For (A) and (C), single asterisk (*) $p < 0.05$ and triple asterisk (***) $p < 0.001$ compared to vehicle group by unpaired Student's t-test. For (B) and (D), the dotted line indicates the Least Significant Change (LSC) in pMET:MET ratio from the vehicle-treated group of 45% ; changes larger than this are attributed to drug effect.

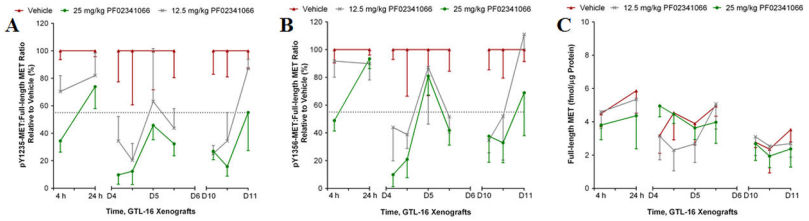

Figure 4. Reduction of GTL-16 tumor growth and MET phosphorylation by PF02341066.

(A) pY1235-MET:MET ratio and **(B)** pY1356-MET:MET ratio during daily treatment with PF02341066. Tumor samples were analyzed at 4 and 24 h after dose 1, then 4, 12 and 24 h after dose 4 (D4), 12 h after dose 5 (D5), and 4, 12, and 24 h after dose 10 (D10). Mean ± SD, all groups n = 2-6 per dose per time point. The dotted line indicates the LSC in pMET:MET ratio from the vehicle-treated group of 45%; changes larger than this are attributed to drug effect. **(C)** Absolute levels of full-length MET plotted over time following daily doses of 12.5 and 25 mg/kg PF02341066 or vehicle; data normalized to extracted protein.

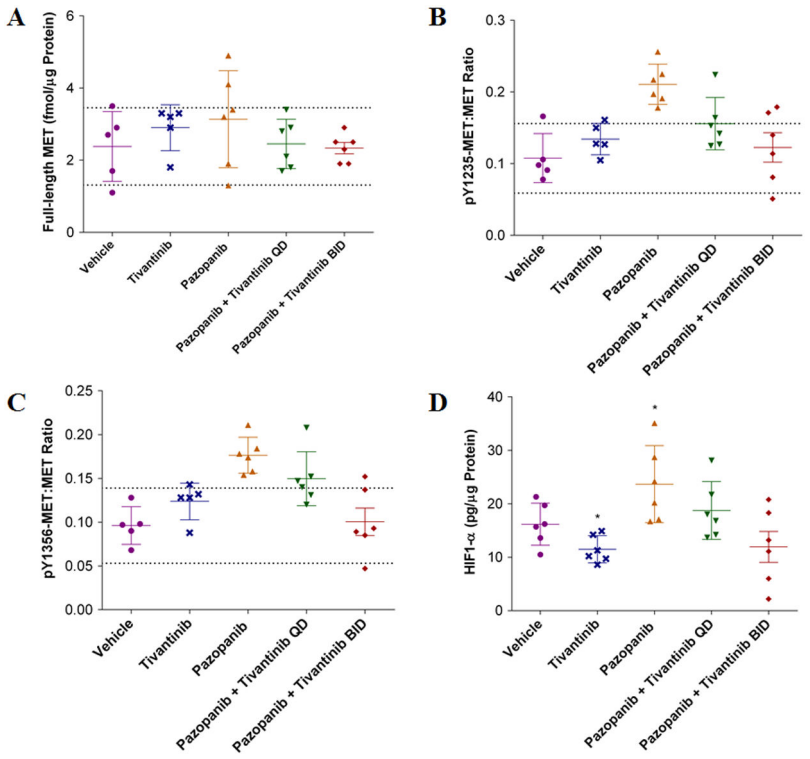

Figure 5. Treatment of SNU5 gastric cancer xenografts with the VEGFR inhibitor pazopanib activates MET.

Full-length MET, pMET:MET ratios, and HIF-1α levels were measured on day 8 of treatment with vehicle, tivantinib or pazopanib alone, or the combination of pazopanib + tivantinib (QD or BID) in combination. **(A)** Absolute levels of full-length MET, **(B)** pY1235-MET:MET ratio, and **(C)** pY1356-MET:MET ratio. The dotted line indicates the LSC in pMET:MET ratio from the vehicle-treated group of 45%; changes larger than this are attributed to drug effect. **(D)** HIF-1α levels were measured in extracts generated from xenograft tumor quadrants. All graphs plotted mean ± SD, all groups n = 5-6 per dose per time point. Single asterisk (*) $p < 0.05$ compared to vehicle group.

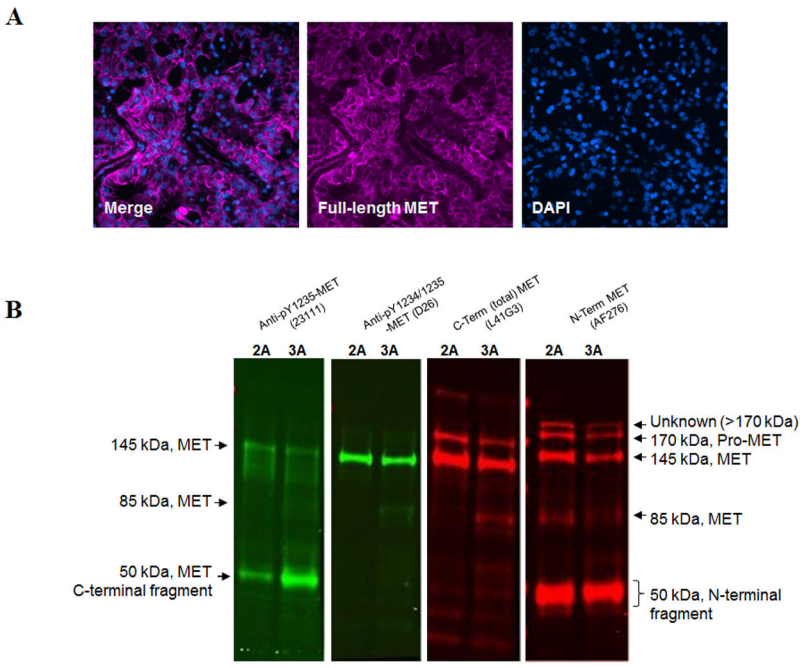

Figure 6. MET assessment in core biopsies of a surgically resected HPRC tumor.

(A) Immunofluorescence staining of a section from a formalin-fixed, paraffin-embedded core needle specimen of a resected HPRC tumor. Merged and individual fluorescent images of N-terminus MET staining with AF276 antibody (pink; primarily membrane) and nuclear staining with DAPI (blue). Magnification, 40×. **(B)** Tissue extracts of HPRC core biopsies sequentially analyzed by Western blot using antibodies against pY1235-MET (clone 23111), pY1234/1235-MET (clone D26), N-terminal MET (AF276), and C-terminal MET (L41G3). Anti-pY1235-MET primarily recognizes a truncated, C-terminal form of MET, while anti-pY1234/1235-MET recognizes mostly full-length MET. In addition, a minor protein band >170 kDa was detected with the MET N-terminal specific antibody, which is not recognized by the other MET antibodies. The MET N-terminal-specific antibody also recognizes a truncated N-terminal MET fragment. Sample load was 25-50 μg protein per gel lane. The numbers (“2” and “3”) indicate the specimen numbers described in Table 2.